International Journal of Minerals, Metallurgy and Materials
Volume 19, Number 2, Feb 2012, Page 173
DOI: 10.1007/s12613-012-0534-1

Preparation of high emissivity $NiCr_2O_4$ powders with a spinel structure by spray drying

Xu-dong Cheng[1)], *Jie Min*[2)], *Zhen-qi Zhu*[2)], *Wei-ping Ye*[2)]

1) State Key Laboratory of Advanced Technology for Materials Synthesis and Processing, Wuhan University of Technology, Wuhan 430070, China
2) School of Materials Science and Technology, Wuhan University of Technology, Wuhan 430070, China

(Received: 5 December 2010; revised: 12 January 2011; accepted: 25 January 2011)

Abstract: Spray-drying was used to produce the high emissivity $NiCr_2O_4$ powders with a spinel structure. Preliminary investigations focused on fabricating the high emissivity powders for infrared radiation coatings and finding the relationship between microstructure and emissivity. The $NiCr_2O_4$ powders were characterized for composition, microstructure, and infrared emissivity by X-ray diffraction (XRD), scanning electron microscopy (SEM), infrared radiant instrument, and Fourier transform infrared spectra (FT-IR). Thermogravimetry and differential thermal analysis show that the appropriate baking temperature for $NiCr_2O_4$ powder preparation is about 1200°C. The emissivity measurement and FT-IR spectra show that, because of the special spinel structure, the $NiCr_2O_4$ powders have a high emissivity about 0.91. Spray-drying is a suitable method to produce the high emissivity ceramic powders.

Keywords: emissivity; infrared radiation; spray drying; powders; ceramic materials; nickel compounds; chromium compounds

1. Introduction

Recently, high infrared emissivity coatings used in industrial furnaces attract a great attention due to energy savings. So far, composite ceramic coatings with high emissivity, such as SiC-Si_3N_4-Al_2O_3 [1], ZrO_2-Cr_2O_3-SiC [2], and Al_2O_3-SiO_2 [3], have been successfully produced by a brush method. However, both the type and performance of these coatings are still limited [4]. Especially, the adhesion strength of these coatings is weak. Air plasma spraying (APS) is a complex technique to deposit ceramic coatings for wear resistant [5], thermal barrier applications [6], *etc*., which usually have the excellent adhesion strength. However, there are few reports about preparing high infrared radiation coatings by APS methods. Obviously, controlling and optimizing the powder morphology seem to be the first step to enhance the emissivity of plasma sprayed infrared radiation coatings. Spray-drying is an effective method to prepare dry particles which is widely used to produce the granulated feed powders.

On the other hand, spinel ceramic materials with the general formula of AB_2O_4 have been widely used in industrial applications, such as metallurgical [7], electronic apparatus [8], and chemical industrial fields [9]. It is well known that both NiO and Cr_2O_3 have a high emissivity, which indicates that $NiCr_2O_4$ probably has a high emissivity too.

$NiCr_2O_4$ spinel infrared radiation powders were fabricated in the study. To characterize the powders and find the relationship between emissivity and experimental parameters, granularity analyses, X-ray diffraction (XRD), scanning electron microscopy (SEM), thermogravimetry (TG), differential thermal analysis (DTA), Fourier transform infrared spectra (FT-IR), and infrared radiation property measurement were utilized.

2. Experimental

The infrared radiation powders were prepared by spray drying in this study. At first, several raw materials, including metal oxides (Cr_2O_3, NiO, Al_2O_3, SiO_2, MnO_2, TiO_2, and Fe_2O_3), organic binder, and deionized water, were mixed in proportion to become a well-ground slurry. Then, in a spray dry tower, the slurry was sprayed to agglomerate to be powders. The composition of raw powders is shown in Table 1.

Corresponding author: Zhen-qi Zhu E-mail: hubeizhq@163.com

Table 1. Composition of compound powder wt%

Cr_2O_3	NiO	Al_2O_3	TiO_2	SiO_2	Fe_2O_3	MnO_2
38.6	40.1	3.3	6.3	5.1	3.3	3.3

Table 2 shows operating parameters for preparing the spray-dried spinel powders. The sprayed powders were chosen with a granularity of 45-75 μm and baked in the air. DTA and TG analyses were carried out with the dried powders in a thermal analyzer (CN8078B2) at a heating rate of 20 K/min and an air flow rate of 10 L/min. High-purity α-alumina was utilized as a reference material. The phase structures were identified by XRD (D/MAXIII) at a scanning speed of 0.02°/s. Microstructural observation of the coatings was performed by SEM (JSM-5610LV). The infrared radiation characteristics were examined by an infrared radiation instrument (IRE-2,) at 600°C. The FT-IR spectra were measured on a Nicolet 60-SXB FT-IR spectrometer with a resolution of 0.02 cm^{-1} over a spectral range of 400-4000 cm^{-1}.

Table 2. Operating parameters for preparing the spray-dried spinel powders

Operating Parameters	value
Inlet temperature / °C	170-190
Outlet temperature / °C	30-40
Feed pump speed / ($r\cdot min^{-1}$)	700-800
Atomizing disk speed / ($r\cdot min^{-1}$)	200-300

3. Results and discussion

3.1. Thermodynamic analysis

Essential thermodynamic analysis was used to infer possible products during the experiment. First, the phase diagram of Cr_2O_3-NiO was used to determine the appropriate baking temperature. From the NiO-Cr_2O_3 phase diagram, the sample can transform into liquid phase beyond 2000°C, hence, the preparatory baking temperature range is about 1700-1800°C. Second, using relevant thermodynamic data, the free energy changes ($\Delta G=A+BT$) of each reaction can be calculated as a function of temperature (T), as shown in Table 3. The standard molar Gibbs energy of $NiCr_2O_4$ formation agreed with the result calculated by Rudnyi *et al.* [10]. It showed that $NiCr_2O_4$ was the primary product because of its lowest ΔG. With the increase of temperature, the trend of forward reaction ($NiO+Cr_2O_3 \rightarrow NiCr_2O_4$) decreased instead, which meant that the excessive temperature was harmful for the production. After comprehensive consideration, the baking temperature of feedstock powders was determined as 900-1200°C.

Table 3. Free energy changes ($\Delta G=A+BT$) of reactions at different temperatures

Reaction	Free energy changes		Temperature range / °C
	A / ($J\cdot mol^{-1}$)	B / ($J\cdot K\cdot mol^{-1}$)	
$NiO+Cr_2O_3=NiCr_2O_4$	−53600	8.40	727-1227
$NiO+Fe_2O_3=NiFe_2O_4$	−19900	−3.77	582-1427
$NiO+Al_2O_3=NiAl_2O_4$	−4180	−12.55	700-1300
$2NiO+SiO_2=Ni_2SiO_4$	−15500	9.20	25-1545
$NiO+TiO_2=NiTiO_3$	−18000	8.40	477-1427

Note: A and B are the coefficients for the free energy changes.

3.2. TG-DTA analysis

DTA and TG analyses are carried out from 25 to 1200°C to find the elimination temperature of volatile phases and determine the baking temperature, as shown in Fig. 1. It reveals that the major part of weight loss occurs below 300°C. There is a weak broad endothermic peak below 400°C in the DTA curve, which mainly corresponds to the evaporation of residual free water and the decomposition of residual organic binder. Because the processes of evaporation and decomposition are continuous, the endothermic peak is broad and weak. The DTA analyses show two obvious exothermic peaks at 639.8 and 1039.8°C, which correspond to the crys-

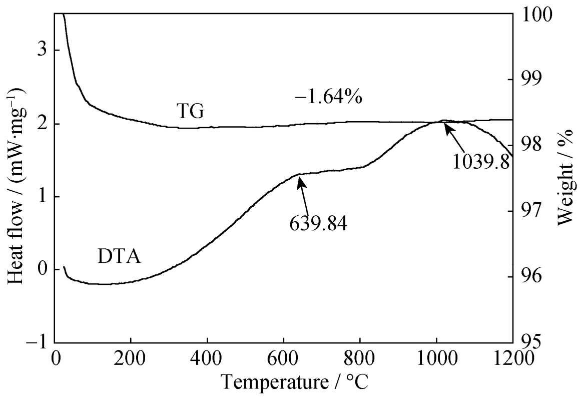

Fig. 1. Thermogravimetry (TG) and differential thermal analysis (DTA).

tallizing of Cr_2O_3 and the synthesis reaction of $NiO+Cr_2O_3 \rightarrow NiCr_2O_4$, respectively. The result is confirmed by the fact that the baking temperature is beyond 900°C for producing $NiCr_2O_4$ phase.

3.3. XRD analysis

XRD patterns of the sample at different baking temperatures are shown in Fig. 2. Except NiO and Cr_2O_3, no spinel structure is found when the baking temperature is lower than 500°C, because the baking temperature is too low to start the reaction. When the baking temperature is beyond 900°C, $NiCr_2O_4$ of spinel structure is successfully generated. The diffraction peaks are consistent with the standard JCPDS cards of $NiCr_2O_4$, Cr_2O_3, and NiO, respectively, and it is very surprised to find that the samples are mainly composed of $NiCr_2O_4$ and Cr_2O_3 phase but without NiO. Moreover, with increasing temperature, the content of Cr_2O_3 in samples decreases, while the content of $NiCr_2O_4$ increases. This suggests that the adequate reaction between raw materials leads to the decrease of NiO content, which is why there is no diffraction peak of NiO beyond 900°C. This result was contrary to the conclusion in Ref. [10], which reckoned that the activity of NiO was equal to that of Cr_2O_3. In fact, it was only an ideal theoretical condition in equilibrium state which was different from the reality. Sloczyński *et al.* [11] prepared $NiCr_2O_4$ with spinel structure by a coprecipitation method using a solution of nickel and chromium nitrates as raw material. Being a wet chemical method, it took a long time (over 50 h) and a complex procedure. In contrast, the solid-phase synthesis is very simple and effective.

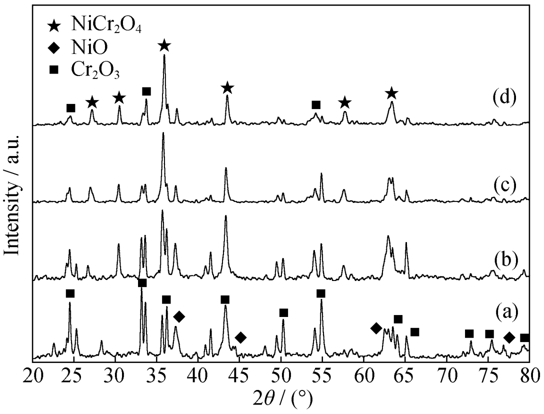

Fig. 2. X-ray patterns of powders at different baking temperatures: (a) 500°C ; (b) 900°C ; (c) 1000°C ; (d) 1200°C.

Owing to the cubic structure (space group: *Fd*3*m*), $NiCr_2O_4$ with spinel structure has a high emissivity close to 0.90 and a stable phase especially at high temperature. It is well known that there are two types of spinel structures according to the distribution of cations. In the normal spinel, the spinel structure contains two cation sites for metal cation occupancy. There are 8 A-sites (Ni^{2+}) in which metal cations are tetrahedrally coordinated with oxygen anions and 16 B-sites (Cr^{3+}) which possess the octahedral coordination. On the contrary, in the inverse spinel, half of the B ions (Cr^{3+}) enter the fourfold coordination with the consequent migration of A ions (Ni^{2+}) to the octahedral sites. Unfortunately, the structure type of as-prepared $NiCr_2O_4$ can not be determined just by XRD. However, this problem can be solved if a more precise examination is considered.

3.4. FT-IR analysis

Infrared spectra are of great importance in resolving the problem of order/disorder in the spinel structure which is closely related with the emissivity. Based on the factor-group analysis, the group theory predicts that in the cubic spinel, four infrared active vibrations should be present [12]. Two intense bands are at 600-400 cm^{-1}, the other two are at low frequencies of 300-200 cm^{-1}, but the latter are generally difficult to record. Both the normal and inverse spinels have the same absorption bands. Fig. 3 shows the in-

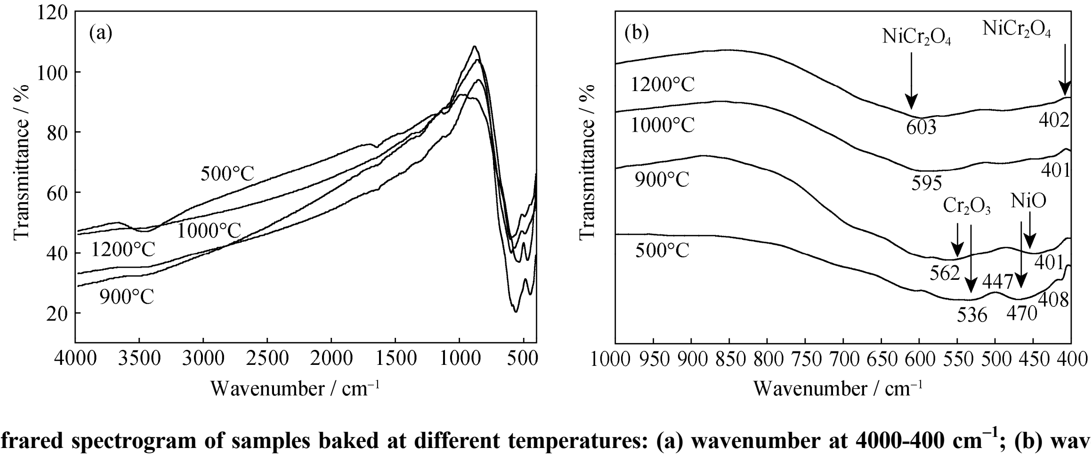

Fig. 3. Infrared spectrogram of samples baked at different temperatures: (a) wavenumber at 4000-400 cm^{-1}; (b) wavenumber at 1000-400 cm^{-1}.

frared spectrum of spray-drying powders after being treated at different baking temperatures in the range of 4000-400 cm^{-1}. As shown in Fig 3(a), when the baking temperature is 500°C, several spectrum bands of metal oxides appear, and there are no characteristic bands of $NiCr_2O_4$ spinel. The peak at 470 cm^{-1} in Fig. 3(b) is undoubtedly assigned to the Ni–O stretching as reported in Refs. [13-14]. The weak peaks at 3455 cm^{-1} and 1641 cm^{-1} in Fig. 3(a) are assigned to the O–H stretching and bending vibration belonging to the adsorbed water, respectively [15]. The peak at 536 cm^{-1} in Fig. 3(b) is ascribed to Cr–O vibrations [16]. When the synthesis temperature is up to 1000°C, two bands emerge at 595 cm^{-1} and 401 cm^{-1} in Fig 3(b). They are attributed to two kinds of $[CrO_6]$ octahedral Cr–O–Cr non-symmetric stretching vibration bands [17]. These two strong absorption bands are typical of inverse spinel structure. But recently, it tends to be accepted that the complex vibration of the entire lattice is atomic displacement which contributes to the infrared spectra of spinel phases. Moreover, the absorption bands vary considerably with the compound, and this depends on the mass, charge, and chemical property of ions. To sum up, the mechanism of absorption bands is under controversy. Nevertheless, it can be concluded that spinel structure is partially formed at 900°C, but there is still a great amount of Cr_2O_3 which is consistent with XRD results.

3.5. Particle morphology analysis

Powder morphology and characteristics have significant effect on the thermal spraying. They can influence the coating characteristic through the microstructure. Three kinds of samples with different particle sizes (120-280 mesh, 280-400 mesh, and over 400 mesh) were achieved using a sifter and recorded as A, B, and C in sequence. Table 4 shows the character parameters of samples with different particle sizes.

Table 4. Character parameters of samples with different particle sizes

Sample	A	B	C
Average size / μm	15.46	14.48	12.94
Specific area / ($m^2 \cdot g^{-1}$)	0.1683	0.2266	0.2419
Max. size / μm	38.97	31.23	26.12
Min. size / μm	3.49	3.38	3.28

Fig. 4 shows the typical SEM images of sample C. It can be seen that the spray-drying powders mainly consist of approximately spherical grains with the diameter range of 10-50 μm, and no agglomeration is found. Partially, there are lots of holes in the spherical grains, and the surface is very rough, as shown in Fig. 4(b). The spherical particles cause the low inter-particle friction and lead to the excellent flow ability. In comparison with the traditional powders, the spherical powders have many advantages, such as good flow ability, uniform composition, and morphology. For the plasma spraying process in particular, it can maintain the plasma stream with a steady speed, which is very useful for melting and deposition efficiently. Yu *et al.* [18] proposed a theoretical model to interpret the effect of porosity on emissivity. According to the results, a high porosity in the coating is helpful for a high emissivity. As for the influence of roughness on emissivity, the increase of roughness is sure to increase the emissivity in the intermediate region. From above, spray drying is an effective tool to fabricate the infrared radiation powders.

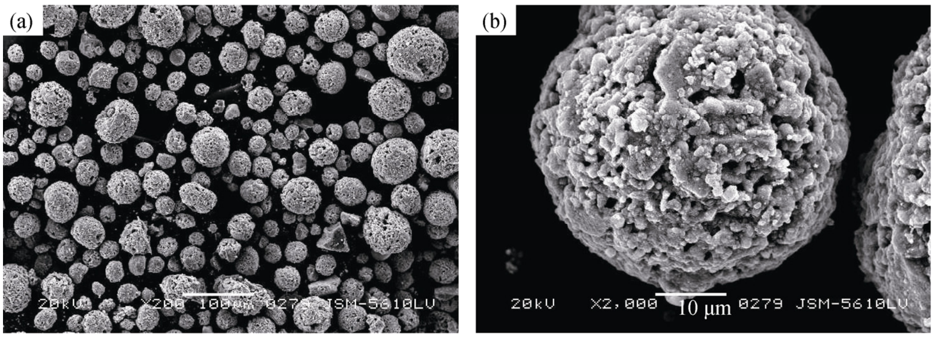

Fig. 4. SEM images of sample C: (a) low magnification; (b) high magnification.

3.6. Emissivity performance

Infrared emission is a primary concern for energy conservation among the radiative properties. For solid powders, the emissivity is determined by many factors, such as chemical composition, crystal structure, and chemical bonding characteristics. Fig. 5 gives the total emissivity of samples baked at different temperatures with the size of sample C. As shown in Fig. 5, the powder emissivity has a maximum value of ~0.90, indicating that $NiCr_2O_4$ has a larger emissivity than NiO (0.89) and Cr_2O_3 (0.83). Thus, the

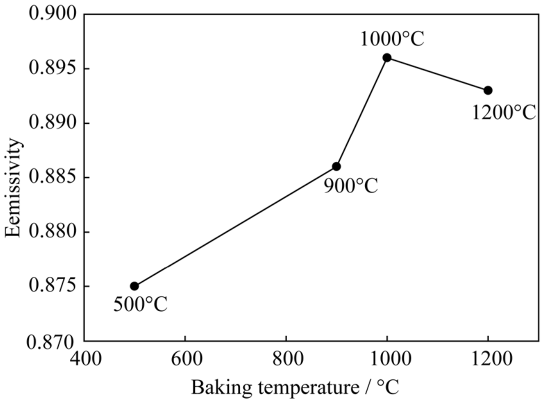

Fig. 5. Relationship between emissivity and baking temperature of sample C.

emissivity is the smallest without $NiCr_2O_4$ spinel formation at low temperature (*i.e.* 500°C). However, with the increase of baking temperature, the emissivity of the sample increases firstly, then decreases after 1000°C lightly.

The powder emissivity is determined by many factors as above. These factors play a complex and flexible role in influencing the emissivity. For example, composite materials can improve the emissivity. At the baking temperature of 900°C, the sample is the mixture of $NiCr_2O_4$, NiO, and Cr_2O_3 with a minimum content of spinel, while the sample is in shortage of NiO at 1200°C, and has a lower content of Cr_2O_3 with a maximum content of spinel. Even though the sample at 1200°C has more $NiCr_2O_4$ than the sample at 1000°C, the emissivity declines on the contrary due to the shortage of NiO. Accordingly, the highest content of $NiCr_2O_4$ at 1200°C may not mean the highest emissivity. Nevertheless, it still can prove that $NiCr_2O_4$ powders with spinel structure have a high emissivity of about 0.91, probably higher than that of Cr_2O_3 or NiO as presumed. Considering the stability at high temperature, it can predict that $NiCr_2O_4$ with spinel structure has a wide application prospect. Furthermore, other spinel compounds probably also have a high emissivity due to their spinel structure. As for the influence of particle size on emissivity, the experimental results indicate that particle size influences the emissivity slightly, as shown in Table 5.

Table 5. Emissivity of samples baked at 1000°C with different sizes

Sample	A	B	C
Emissivity	0.882	0.890	0.896

The quantum theory shows that the radiation emission is the interaction result of molecular transition dipoles and oscillating electric fields essentially, which is related with the vibration of crystal structure. The stronger the lattice vibration is, the greater the emissivity will be. Doping is an effective way to improve the lattice vibration. Using Mn^{2+} and Fe^{3+} ions instead of Ni^{2+} and Cr^{3+} ions in the spinel structure properly increases the anharmonicity of lattice vibration, which results in the improvement of infrared radiation properties. Another consequence caused by dopants is the crystal distortion due to the different ion radii. When Mn^{2+} and Fe^{3+} ions are incorporated into the spinel structure, the order degree of Ni/Cr in the crystal structure decreases due to the different radii, as a result, leading to crystal structure distortion. The substitution of Ni^{2+} cations can lead to a significant modification of the NiO_4 tetrahedron, which is simply shown by the variation of Ni–O bond length. This decreases the symmetry of lattice vibration in turn, and enhances the effects of the anharmonic vibration of polar lattices, coupled action of phonons, and phonon combination radiation. Therefore, the emissivity should be enhanced by doping MnO_2 and Fe_2O_3.

4. Conclusion

High emissivity $NiCr_2O_4$ powders with a spinel structure were fabricated by a spray-drying method. From thermal analysis, an appropriate baking temperature range of 900-1200°C is necessary for the process. Spray-drying is a suitable method to fabricate the high emissivity ceramic powders, because the powders generally have the rough and porous surfaces. The high emissivity about 0.91 is mainly attributed to the spinel structure, which is very useful for the application at high temperature. Furthermore, the emissivity is affected by many factors, such as chemical composition, crystal structure, and chemical bonding characteristics. In sum, the further work will be required to find the relationship between emissivity and microstructure for $NiCr_2O_4$ spinel.

Acknowledgments

The authors would like to thank Yu Zeng and Ping Ye of China National Infrared & Industrial Electrothermal Products Quality Supervision & Testing Centre for the infrared normal total emissivity measurements of coatings.

References

[1] M. Falz and G. Leonhardt, PVD coatings with high IR emissivity for high temperature applications of Co-based alloys, *Surf. Coat. Technol.*, 61(1993), No.1-3, p.97.

[2] Z.G. Dan, D.Q. Cang, H.M. Zhou, and Y.B. Zong, Microstructure and properties of high emissivity coatings, *J. Univ. Sci. Technol. Beijing*, 15(2008), No.5, p.627.

[3] K. Shimazaki, M. Imaizumi, and K. Kibe, SiO_2 and Al_2O_3/SiO_2 coatings for increasing emissivity of Cu(In, Ga)Se_2 thin-film solar cells for space applications, *Thin Solid Films*, 516(2008), No.8, p.2218.

[4] X.D. He, Y.B. Li, L.D. Wang, *et al.*, High emissivity coatings for high temperature application: progress and prospect, *Thin Solid Films*, 517(2009), No.17, p.5120.

[5] E.P. Song, B. Hwang, S. Lee, *et al.*, Correlation of microstructure with hardness and wear resistance of stainless steel blend coatings fabricated by atmospheric plasma spraying, *Mater. Sci. Eng. A*, 429(2006), No.1-2, p.189.

[6] A. Nusair Khan, J. Lu, and H. Liao, Effect of residual stresses on air plasma sprayed thermal barrier coatings, *Surf. Coat. Technol.*, 168(2003), No.2-3, p.291.

[7] M. Bavand-Vandchali, H. Sarpoolaky, F. Golestani-Fard, and H.R. Rezaie, Atmosphere and carbon effects on microstructure and phase analysis of in situ spinel formation in MgO-C refractories matrix, *Ceram. Int.*, 35(2009), No.2, p.861.

[8] P.E. Lippens, M. Womes, P. Kubiak, J.C. Jumas, and J. Olivier-Fourcade, Electronic structure of the spinel $Li_4Ti_5O_{12}$ studied by ab initio calculations and X-ray absorption spectroscopy, *Solid State Sci.*, 6(2004), No.2, p.161.

[9] H. Reverón, D. Gutiérrez-Campos, R.M. Rodríguez, and J.C. Bonassin, Chemical synthesis and thermal evolution of $MgAl_2O_4$ spinel precursor prepared from industrial gibbsite and magnesia powder, *Mater. Lett.*, 56(2002), No.1-2, p.97.

[10] E.B. Rudnyi, E.A. Kaibicheva, L.N. Sidorov, M.T. Varshavskii, and A.N. Men, (Ion+molecule) equilibrium technique applied to the determination of the activities of Cr_2O_3 and NiO. Standard molar Gibbs energy of formation of $NiCr_2O_4$, *J. Chem. Thermodyn.*, 22(1990), No.7, p.623.

[11] J. Sloczyński, J. Ziólkowski, B. Grzybowska, *et al.*, Oxidative dehydrogenation of propane on $Ni_xMg_{1-x}Al_2O_4$ and $NiCr_2O_4$ Spinels, *J. Catal.*, 187(1999), No.2, p.410.

[12] E. Wolska, P. Piszora, K. Stempin, *et al.*, X-ray powder diffraction study of cation distribution and the $Fd3m \rightarrow P4_132$ symmetry reduction in $Li_{0.5}Fe_{2.5}O_4/LiMn_2O_4$ spinel solid solutions, *J. Alloys Compd.*, 286(1999), No.1-2, p.203.

[13] F. Davar, Z. Fereshteh, and M. Salavati-Niasari, Nanoparticles Ni and NiO: Synthesis, characterization and magnetic properties, *J. Alloys Compd.*, 476(2009), No.1-2, p.797.

[14] F. Liu, J. Lu, J. Shen, and Z. Zhang, Preparation of mesoporous nickel oxide of sheet particles and its characterization, *Mater. Chem. Phys.*, 113(2009), No.1, p.18.

[15] S.M. Abo-Naf, M.S. El-Amiry, and A.A. Abdel-Khalek, FT-IR and UV-Vis optical absorption spectra of γ-irradiated calcium phosphate glasses doped with Cr_2O_3, V_2O_5 and Fe_2O_3, *Opt. Mater.*, 30(2008), No.6, p.900.

[16] M. Ocaña, Nanosized Cr_2O_3 hydrate spherical particles prepared by the urea method, *J. Eur. Ceram. Soc.*, 21(2001), No.7, p.931.

[17] J.L. Gunjakar, A.M. More, K.V. Gurav, *et al.*, Chemical synthesis of spinel nickel ferrite ($NiFe_2O_4$) nano-sheets, *Appl. Surf. Sci.*, 254(2008), No.18. p.5844.

[18] H.J. Yu, G.Y. Xu, X.M. Shen, *et al.*, Effects of size, shape and floatage of Cu particles on the low infrared emissivity coatings, *Prog. Org. Coat.*, 66(2009), No.2, p.161.